

# Shock Reflection Detonation Initiation Studies for Pulse Detonation Engines

B. de Witt\* and G. Ciccarelli†

*Queen's University, Kingston, Ontario K7L 3N6, Canada*

and

F. Zhang‡ and S. Murray‡

*Defence Research and Development Canada–Suffield, Alberta T1A 8K6, Canada*

A new technique to initiate a detonation wave via the interaction of a high-speed flame/shock complex and an obstacle is investigated. Experiments were performed in which a flame was ignited at the closed end of a tube partially filled with orifice plates leading up to the “reflecting” obstacle. Two different types of obstacles were tested. The obstacles include assemblies consisting of a circular plate followed by an orifice plate and a cone followed by an orifice plate. The flame accelerates in the orifice plate laden section of the tube to a high velocity producing a shock wave ahead of it. This shock wave interacts with the obstacle by first colliding with the leading central blockage, that is, the circular plate or the cone, and then reflecting off the orifice plate. Shock reflection produces a region of high temperature and pressure that ignites the reactants, which under certain circumstances, can initiate a detonation wave. The experiments were performed with stoichiometric ethylene–oxygen mixtures at atmospheric conditions with nitrogen dilution. The nitrogen dilution was varied, and the maximum nitrogen dilution that resulted in detonation initiation, that is, the critical mixture, was found. For experiments performed with the circular plate reflector obstacle, detonation initiation was observed for mixtures with a nitrogen–oxygen concentration ratio up to 3.98. In experiments with the cone reflector obstacle, detonation initiation occurred for less reactive mixtures, that is, mixtures with a nitrogen-to-oxygen concentration ratio of up to 4.33. Additional experiments were performed where the cone obstacle was moved closer to the ignition point to find the minimum flame acceleration distance required for detonation initiation. For stoichiometric ethylene–air mixtures, detonation initiation was observed with the cone obstacle located at least 1.36 m from the ignition point. It was found that detonation initiation occurred for the cone reflector when the incident shock wave velocity was above roughly 750 m/s.

## Nomenclature

$c$	=	speed of sound, m/s
$D$	=	inner diameter of detonation tube, m
$d$	=	hole diameter of orifice plate, m
$g$	=	distance between the reflector plate or cone and backup orifice plate, m
$M_i$	=	incident shock wave Mach number
$M_w$	=	Mach stem Mach number
$U$	=	shock wave speed, m/s
$u$	=	postshock velocity in laboratory frame of reference, m/s
$V_w$	=	speed of disturbed boundary region along shock front, m/s
$X$	=	distance from reflector plate where entire Mach stem is affected by diffraction, m
$\beta$	=	ratio of number of moles of nitrogen to number of moles of oxygen
$\delta$	=	cone half angle, deg
$\theta_e$	=	angle separating disturbance boundary of Mach stem and diffracted shock region, deg
$\theta_w$	=	wedge angle, deg
$\tau$	=	chemical induction time, s
$\tau_E$	=	difference in time of arrival of the incident shock wave and the detonation wave, s

$\chi$  = triple-point trajectory, deg

## Introduction

A PULSE detonation engine (PDE) is an unsteady propulsion device that operates cyclically based on the detonation mode of combustion.<sup>1–3</sup> Interest in PDEs has grown primarily due to their simplicity in design. Much like a ramjet, a PDE requires no compressor or turbine to operate. Both turbomachinery are high-maintenance pieces of equipment that make up the bulk of a traditional turbojet engine's weight. It is generally believed that PDEs are thermodynamically more efficient than the steady-state propulsion systems currently in use that operate via constant pressure combustion.<sup>4</sup> One of the key technical hurdles that must be overcome for PDEs to be successful is detonation initiation must be achieved in a distance comparable to the length of existing combustors. Several researchers have investigated the use of an obstacle laden tube for promoting flame acceleration leading to deflagration-to-detonation transition (DDT) for PDE applications. Pinard et al.<sup>5</sup> performed experiments with propane–air in a 15 cm inner-diameter cylindrical tube filled with orifice plates spaced at one tube diameter. They found that DDT occurs after roughly 2 m of flame propagation. Ciccarelli et al.<sup>6</sup> performed experiments in a similar apparatus and looked at the effect of orifice plate blockage and spacing on the initial flame acceleration process. It was determined that optimum flame acceleration was obtained when higher flow blockage plates were used near the ignition point followed by lower blockage plates. Lee et al.<sup>7</sup> performed experiments with a more reactive mixture of ethylene–air in a 44 × 44 mm duct with obstacles consisting of flat plates mounted in a helical pattern. Schlieren, planar laser-induced fluorescence from hydroxyl radicals, and flame emission imaging were used to visualize the shock, reaction zone, and heat release, respectively. In their setup DDT was obtained in just under 1 m. By using obstacles to promote flame acceleration, one pays a performance penalty due to the drag imposed by the obstacles on the internal flow. Cooper

Presented as Paper 2004-3747 at the 40th Joint Propulsion Conference, Fort Lauderdale, FL, 11–14 July 2004; received 4 November 2004; revision received 12 April 2005; accepted for publication 12 April 2005. Copyright © 2005 by the American Institute of Aeronautics and Astronautics, Inc. All rights reserved. Copies of this paper may be made for personal or internal use, on condition that the copier pay the \$10.00 per-copy fee to the Copyright Clearance Center, Inc., 222 Rosewood Drive, Danvers, MA 01923; include the code 0748-4658/05 \$10.00 in correspondence with the CCC.

\*Graduate Student, Mechanical and Materials Engineering, McLaughlin Hall.

†Associate Professor, Mechanical and Materials Engineering, McLaughlin Hall; ciccarel@me.queensu.ca. Member AIAA.

‡Defence Scientist, Military Engineering Section.

et al.<sup>8</sup> found that the impulse produced with an obstacle laden tube was up to 25% lower than the impulse measured in the same tube with no obstacles. Clearly if obstacles are to be used for flame acceleration, the length of the obstacle array must be kept to a minimum to minimize internal drag.

A more rapid transition to detonation can be accomplished if detonation initiation is triggered during flame acceleration by some means. One such mechanism is shock reflection. Shock reflection results in an increase in the pressure and temperature of the gas in the vicinity of the reflecting surface. The rapid chemical energy release triggered in the high-temperature gas produces a strong shock wave that transitions into a detonation wave.<sup>9</sup> Detonation initiation via shock reflection is normally studied using a shock tube consisting of high- and low-pressure sections initially separated by a bursting diaphragm. Clearly a shock tube is not feasible for a PDE initiation system; a more practical method to produce a strong shock wave is via flame acceleration. For a flame ignited at the closed end of a tube, the increase in the specific volume across the flame produces a flow in the unburned gas ahead of the flame. In a smooth-walled tube, flame acceleration occurs in reactive mixtures as a result of the interaction of the flame and the unburned gas turbulent boundary layer. The flame acceleration process can be enhanced by artificially roughening the tube wall with flow obstructions such as orifice plates.<sup>10</sup> The orifice plates produce large-scale flow velocity gradients in the unburned gas that causes the flame to stretch and form additional flame area. This "flame folding" leads to a larger volumetric burning rate and, thus, an increase in the unburned gas velocity. Fine-scale turbulence is also produced in the shear layers that form downstream of the orifice plate hole. This turbulence leads to enhanced burning due to increased mass and energy transport across the flame. A feedback loop is created between the volumetric burning rate and the turbulence in the unburned gas that leads to flame acceleration.<sup>11</sup> In effect, the flame behaves like a porous piston that pushes the unburned gas, producing compression waves that propagate away from the flame. As the flame accelerates to velocities greater than the speed of sound of the unburned gas, the compression waves coalesce and form a shock wave. This shock wave can interact with an obstacle, and the reflected shock can initiate a detonation under suitable conditions.

A shock wave that collides with a surface can undergo regular or Mach reflection depending on the angle of incidence of the shock wave on the reflecting surface.<sup>12</sup> In regular reflection, the reflected shock wave moves away from the reflecting surface reinforcing the compression achieved by the incident shock wave. The shock reflection further raises the thermodynamic parameters downstream. In Mach reflection, a shock wave traveling parallel to the reflecting surface, known as a Mach stem, is created. Mach reflection is characterized by the convergence of three shock waves: the incident shock wave, the reflected shock wave, and the Mach stem. The three shock waves intersect at the triple point.<sup>13</sup> A slipstream separates the flow behind the Mach stem and the reflected shock wave. For a given incident shock Mach number and ratio of specific heats, there is a critical shock wave angle of incidence that the reflection changes from the regular to the Mach configuration. For a two-dimensional wedge, the critical angle lies in the range of 45–50 deg (Ref. 13). If the wedge angle is less than the critical wedge angle  $\delta_c$ , a Mach reflection ensues. The interaction of a planar shock wave with a cone has been studied by Yang et al.<sup>14</sup> These investigators demonstrated that the curvature of the cone compared to the two-dimensional wedge does not affect the critical wedge angle; thus, the cone geometry can be approximated by a wedge with similar shock deflection angle. Whitham formulated a theory for a perfect gas that predicts the Mach stem strength and the trajectory of the triple point.<sup>15</sup>

The highest gas temperature is achieved for normal shock reflection and, thereby, provides the best possibility for detonation initiation. There is a large body of literature on the subject of detonation initiation by shock reflection. One of the earliest and most comprehensive investigations was by Strehlow and Cohen, who studied detonation initiation resulting from the collision of a shock wave and the shock tube endwall.<sup>9</sup> This study demonstrated that detonation initiation is governed by the chemical kinetics of the mixture at the

reflected shock state. Therefore, for a given mixture, the strength of the incident shock wave is the sole parameter influencing the phenomenon. More relevant to the present study are investigations looking at detonation initiation resulting from the collision of a shock wave from a wall-mounted obstacle.<sup>16,17</sup> These studies showed that detonation initiation depends on both the strength of the incident shock wave as well as the height of the obstacle. The gas bounded by the reflected shock and the obstacle surface is at a high pressure and temperature. The pressure and temperature are progressively reduced by expansion waves originating at the obstacle free edge that travel across the obstacle face. Therefore, the height of the obstacle governs the expansion time of the reflected shock compressed gas adjacent to the obstacle. Detonation initiation occurring as a result of shock focusing has also been studied.<sup>18</sup> This phenomenon has received considerable attention by the PDE research community because detonation initiated can be achieved by a weaker incident shock wave.<sup>19,20</sup>

The objective of any study dealing with detonation initiation for a PDE application is to initiate a detonation wave in a tube at an axial distance as close as possible to the ignition point. In this study, a tube filled with turbulence generating orifice plates is used to accelerate a flame that consequentially produces a shock wave. The shock wave interacts with an obstacle resulting in the initiation of a detonation wave. Two obstacle configurations were tested. The obstacles are designed to focus the shock wave before colliding with an orifice plate. The experiments were performed with stoichiometric ethylene–oxygen mixtures at atmospheric conditions with nitrogen dilution. The nitrogen dilution was varied to find the least reactive mixture that resulted in detonation initiation.

## Experimental Details

Experiments were performed in a 3.1-m-long, 14-cm internal diameter detonation tube. A schematic of the apparatus is shown in Fig. 1b. The first 1.36 m of the tube is referred to as the flame acceleration section. This part of the tube is filled with orifice plates equally spaced at 15.2 cm. The orifice plates are characterized by the flow area blockage ratio (BR), which is defined as

$$BR = 1 - (d/D)^2 \quad (1)$$

where  $d$  is the orifice plate hole diameter and  $D$  is the inner diameter of the tube. Most of the experiments were performed using orifice plates with a 10.7-cm hole diameter, which yields a blockage ratio of 0.42. Over this first section of the tube, the flame accelerates to a velocity on the order of 1000 m/s, and by the end of the flame acceleration section, the flame is preceded by a shock wave. To decouple the flame and the shock wave, a smooth transition section exists between the last flame acceleration orifice plate and the reflecting obstacle. As the flame-shock complex enters this transition section, the flame decelerates due to the absence of turbulence generating obstacles.<sup>21</sup>

The reflecting obstacles tested include a reflector plate assembly and a reflector cone assembly (Fig. 1b). The reflector plate assembly consists of a circular plate followed by an orifice plate. The circular plate is 9.65 cm in diameter, and the orifice plate has a hole diameter of 5.1 cm. Both plates have sharp corners and are 1.27 cm thick. The gap spacing  $g$  between the plate and the orifice plate was varied between 2.54 and 5.1 cm. Both the circular plate and the orifice plate provide normal reflecting surfaces for the shock wave propagating through the transition section of the tube. The shock diffraction around the circular plate also produces an imploding shock wave on the back side of the plate. In the case of the cone assembly, the shock wave strengthens as it propagates through the area contraction around the cone. This stronger shock wave reflects off the orifice plate generating a high-pressure and high-temperature region in the gap just ahead of the orifice plate. As a result of the shock strengthening, it is hypothesized that this configuration will be more favourable for detonation initiating compared to the reflector plate assembly. The cone apex angle is 45 deg, and the base diameter is similar to that of the circular plate, that is, 9.65 cm. The base of the cone has a 1.27-cm wide shoulder. The gap spacing between

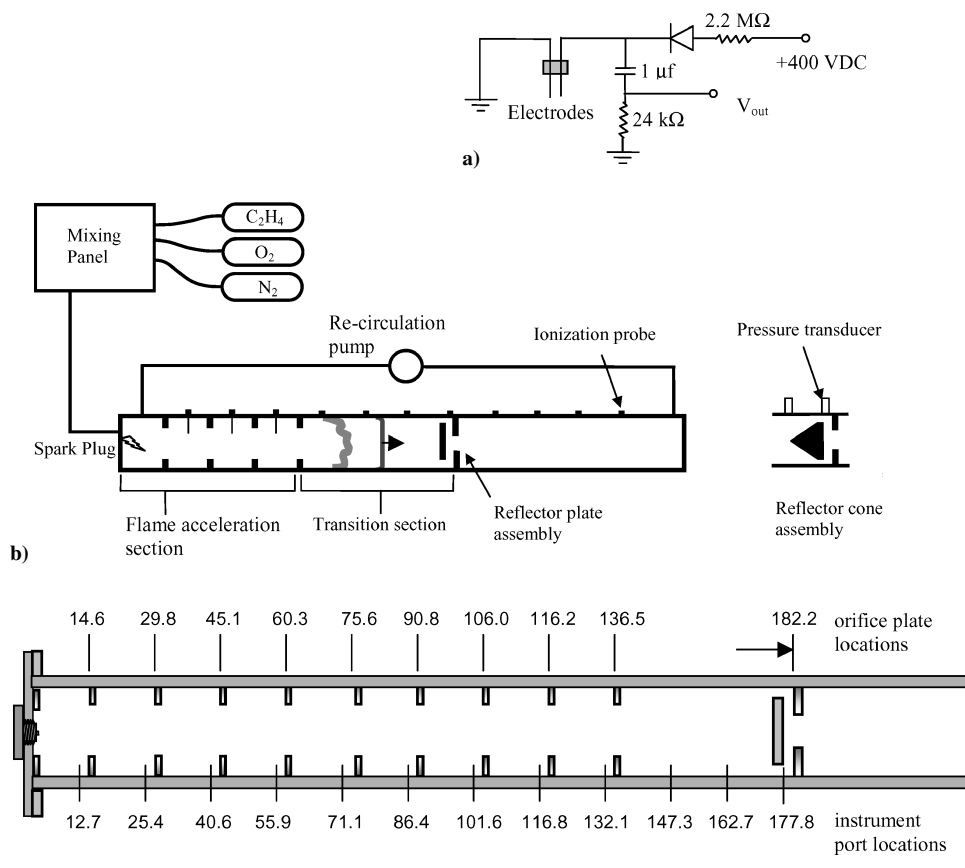


Fig. 1 Experimental apparatus with reflector assembly; all dimensions in centimeters and all distances taken from inner side of endplate.

the cone base and the orifice plate was varied from 2.54 to 5.1 cm, in the same way as the reflector plate assembly. The length of the transition section was varied. For the majority of the experiments the transition section was 0.46 m long.

Experiments were performed with mixtures of stoichiometric ethylene and oxygen, diluted with nitrogen at atmospheric temperature and pressure. For each test, the tube is evacuated to an absolute pressure of less than 0.1 kPa. The mixture is prepared by the method of partial pressures within the tube and then circulated for 20 min to ensure composition homogeneity. The pressure transducer used to measure the vessel fill pressure has an accuracy of 0.25% of full scale, or 0.25 kPa. The mixture reactivity was varied by changing the nitrogen-to-oxygen concentration ratio, denoted by  $\beta$ . Note for standard air  $\beta = 3.76$ . The tube was closed at both ends, and a weak electrical spark of roughly 150 mJ ignited the gas mixture at one end. The spark was produced by a standard automotive inductive spark ignition system powered by a 12-V battery. Flame and shock characteristics are measured via ionization probes and PCB Electronics (Model 113A24) piezoelectric pressure transducers, respectively. The ionization probes located in the flame acceleration section extend to the centerline of the tube. These probes are coaxial in design; the electrodes consist of a 5-mm steel tube and a central 1-mm rod. The space between the two electrodes is filled with epoxy. The rest of the ionization probes are flush mounted with two side-by-side 1-cm-long, 1-mm-diam electrodes protruding into the flow. A schematic of the ionization probe electric circuit is provided in Fig. 1a. The axial locations of the instrument ports and the orifice plates are provided in Fig. 1c.

## Experimental Results

### Reflector Plate Assembly Results

Experiments were performed to investigate the interaction of the flame–shock complex with the reflector plate assembly. The mixture reactivity was varied to study its effect on flame acceleration in

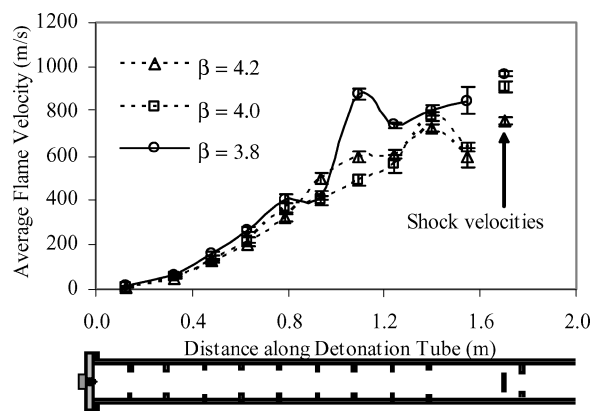


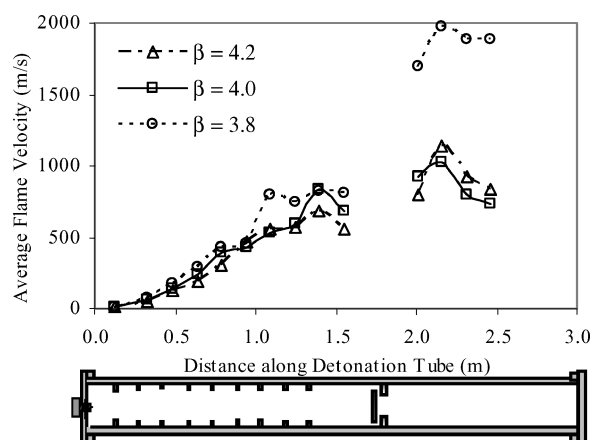
Fig. 2 Effect of mixture reactivity on flame acceleration for  $g = 5.1$  cm reflector plate assembly.

the first section of the tube and the strength of the shock wave produced in the smooth transition section just before the reflector plate assembly. The flame velocity as a function of distance for a gap spacing of 5.1 cm is shown in Fig. 2. Each velocity data point represents the average of three to four tests, and the vertical error bar represents the standard deviation of the measurements. Also shown in Fig. 2 is the average shock velocity measured just before the reflector plate assembly via two piezoelectric pressure transducers mounted at 1.63 m and 1.78 m from the ignition end of the tube.

For the mixture with  $\beta = 3.8$ , the flame accelerates smoothly up to a distance of roughly 0.8 m, then temporarily decelerates, and then rapidly reaccelerates, eventually reaching a velocity of 800 m/s by the end of the flame acceleration section. This flame velocity perturbation is found to be very repeatable from test to test. For this mixture, no deceleration of the flame is observed in the

**Table 1 Shock-flame separation distance within the smooth transition section just before reflecting orifice plate**

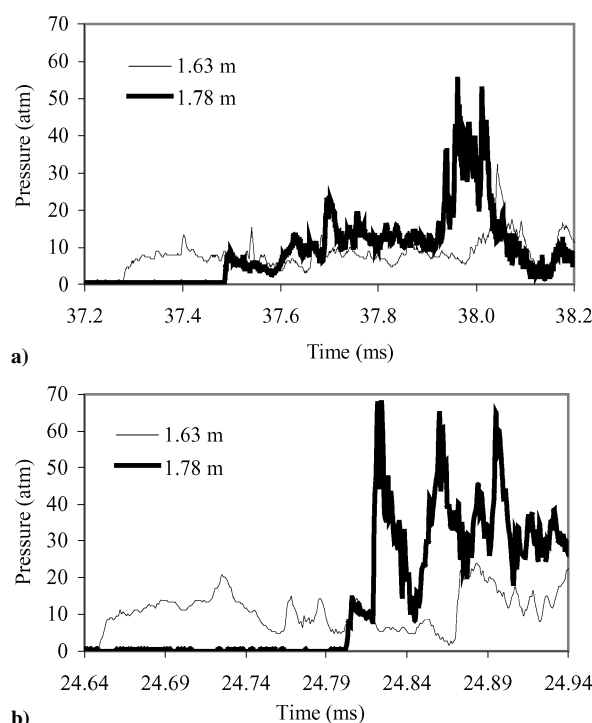
$\beta$	Speed of sound in the products, m/s	CJ detonation velocity, m/s	CJ detonation pressure, atm	Shock–flame separation distance, m	Shock–flame separation time, $\mu$ s
3.8	899	1824	18.4	0.075	93
4.0	893	1809	18.0	0.123	373
4.2	887	1794	17.7	0.139	591
4.5	879	1774	17.3	0.201	1232

**Fig. 3 Effect of mixture reactivity on detonation initiation for  $g = 5.1$  cm reflector plate assembly.**

transition section. The higher maximum flame velocity measured for the mixtures with a lower value  $\beta$  reflects the enhanced flame acceleration due to the higher mixture reactivity. Because the strength of the shock wave is governed by the flame velocity, one would expect a higher shock velocity as well. The average shock velocity measurements are in agreement with this premise, that is, lower  $\beta$  values result in higher average shock velocity measurements in the transition section.

The distance separating the flame and the shock wave ahead of it has an impact on the interaction of the shock wave with the reflector assembly. Based on the measured time of arrival of the flame from the ionization probes and the time of arrival of the shock wave from the pressure transducer, the separation distance between the flame and shock wave was calculated at the instant the shock wave reaches the pressure transducer located at 1.78 m. From this calculation, the time that elapses from when the shock wave reaches the reflector plate to when the flame reaches the reflector plate can be inferred. The shock–flame separation distances and separation times are given for selected mixtures in Table 1. Note for the  $\beta = 4.5$  mixture the shock–flame separation distance and time are extremely large because the flame velocity drops significantly through the smooth transition section.

The objective of these experiments is to determine the effectiveness of the reflector plate assembly to initiate detonation. Figure 3 shows the average flame velocity measurements made at locations along the entire tube. For clarity the data point standard deviation is not shown in Fig. 3. The measured flame velocity before the reflector plate assembly is about 550 m/s for the  $\beta = 4.2$  mixture, 700 m/s for the  $\beta = 4.0$  mixture, and 800 m/s for  $\beta = 3.8$ . The theoretical Chapman–Jouget (CJ) detonation velocity for these mixtures is roughly 1800 m/s (Table 1). The measured velocities after the reflector plate assembly for the  $\beta = 3.8$  mixture is close to the theoretical detonation velocity, which suggests that a detonation wave is initiated at the reflector plate assembly. The flame velocities after the assembly for the  $\beta = 4.0$  and  $\beta = 4.2$  mixtures are well below the theoretical detonation velocity, indicating unsuccessful initiation. The flame velocity approaches 900 m/s, which is close to the speed of sound of the products for a constant pressure combustion process (Table 1). This represents the maximum velocity for steady-

**Fig. 4 Pressure-time history for reflector plate assembly with gap spacing of 5.1 cm; test mixture: a)  $\beta = 4.19$  and b)  $\beta = 3.8$ .**

state flame propagation, and at this velocity the flame is considered choked.<sup>10</sup>

This interpretation of the flame velocity measurements is corroborated by pressure measurements made just before the reflector assembly. Figure 4 shows the pressure-time histories recorded at location 1.63 and 1.78 m from the ignition point for  $\beta = 3.80$  and 4.19 mixtures. Recall, based on the results presented in Fig. 3, detonation initiation occurs for the  $\beta = 3.80$  mixture but not the  $\beta = 4.19$  mixture. The pressure recorded at 1.63 m for the  $\beta = 3.80$  mixture (Fig. 4b) shows a relatively slow initial rise in pressure that is associated with the passage of a forming shock wave with an overpressure of 9 atm. This initial pressure rise is followed by pressure oscillations caused by secondary waves generated by reflections of the shock wave through the orifice plate array. The pressure recorded by the transducer located in the gap between the assembly reflector plate and the orifice plate at 1.78 m shows a more rapid initial rise in pressure with an overpressure of 14 atm. This overpressure corresponds to a Mach 3 shock wave. This shock strength is consistent with a 900-m/s flame velocity, which is typical of a choked flame. The initial pressure rise is immediately followed by a second rapid rise in pressure to 65 atm. This pressure is much greater than the theoretical normal reflected shock pressure of 25 atm for a Mach 3 incident shock wave. One can infer that this strong shock wave is the result of detonation wave initiation in the general area of the reflector plate assembly. The large-pressure pulses that follow are the result of the ensuing detonation wave reflections that occur at the orifice plate and tube wall. This shock is propagating in the combustion products and so the pressure oscillations decay in strength. The pressure-time history recorded for the  $\beta = 4.19$  mixture (Fig. 4a) indicates a more

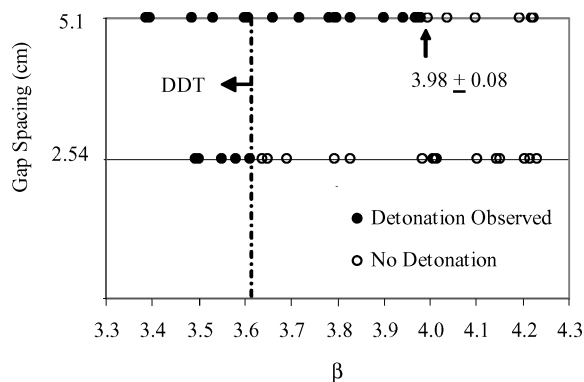


Fig. 5 Detonation initiation results for reflector plate assembly.

modest strength initial shock wave. The measured average shock velocity between the two pressure transducers is 743 m/s. A 55-atm pressure pulse is observed roughly 200  $\mu$ s after the time of arrival of the incident shock wave at the second pressure transducer. The 200- $\mu$ s lag between the time of arrival of the two shock waves is much longer than that observed for the  $\beta = 3.80$  mixture, where the lag is only about 12  $\mu$ s.

Additional experiments were performed with a reflector plate assembly gap of 5.1 cm, and an additional series of experiments was performed with a gap of 2.54 cm. With these various configurations, the mixture reactivity was varied to determine the critical value of  $\beta$ , above which detonation is not observed. The results for the reflecting plate assembly with the two gap spacings are summarized in Fig. 5. The results are categorized according to whether or not a detonation was detected after the reflector plate assembly. For a gap spacing of 2.54 cm, detonation initiation occurs for a critical value of  $\beta = 3.61$ . Based on detailed flame velocity measurements, it was determined that for mixtures with a  $\beta$  value of 3.61 or less detonation initiation occurs as a result of DDT before the reflector plate, that is in the flame acceleration section or in the transition section. Therefore, for these mixtures detonation initiation cannot be attributed to the interaction of the shock wave and the reflector plate assembly. A reflector plate assembly configuration with a gap of 5.1 cm was found to be more effective than the 2.54 cm gap, with detonation initiation occurring in mixtures with a maximum value of  $\beta = 3.98$ . For this critical mixture, the measured average shock velocity just before the reflector plate was 964 m/s.

#### Reflector Cone Assembly Results

Experiments were performed to investigate the performance of the reflector cone assembly with a gap spacing of 2.54 cm. Again the mixture reactivity was varied to study its effect on flame acceleration and the strength of the shock wave produced in the transition section. The flame velocity history in the flame acceleration section and the average shock velocity measured across the cone are shown in Fig. 6. The average shock velocity is based on the shock time of arrival at the pressure transducers located at 1.63 and 1.78 m from the point of ignition. The shock wave strengthens significantly as it propagates across the cone due to the contraction in the annulus cross-sectional area, and thus, the strength of the shock wave reflecting off the orifice plate is higher than that based on the average velocity.

The flame velocity profiles for the  $\beta = 4.0$  and  $\beta = 4.2$  mixtures are very similar. A maximum velocity of 650 m/s is achieved across the last flame acceleration orifice plate. This behavior is similar to that observed in the reflector plate assembly experiments, as shown in Fig. 2. The flame decelerates in the smooth transition section of the detonation tube, but the shock velocity measured across the cone remains high at roughly 900 m/s. This shock velocity is significantly higher than that measured in the reflector plate assembly tests where the shock velocity was under 800 m/s for the  $\beta = 4.2$  mixture. For the  $\beta = 3.8$  mixture, the flame achieves a velocity of roughly 900 m/s by the end of the flame acceleration section, which is close to the choked flame velocity. The average shock velocity achieved for this mixture is 1040 m/s as compared to the sub-1000-m/s

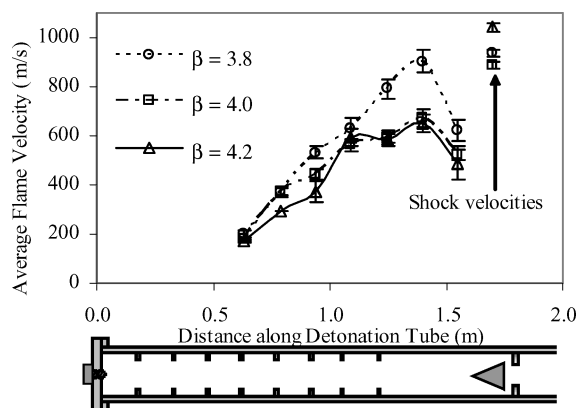


Fig. 6 Effect of mixture reactivity on flame acceleration for  $g = 2.54$  cm reflector cone assembly.

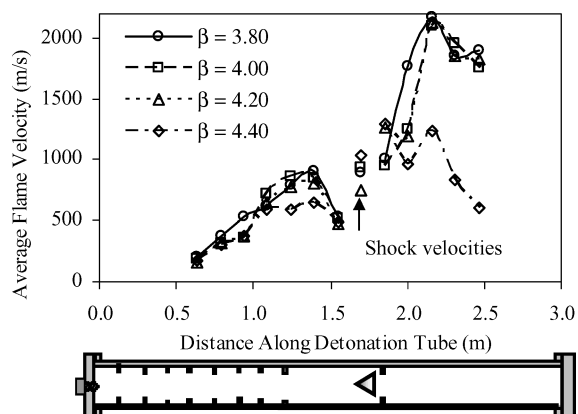


Fig. 7 Effect of mixture reactivity on detonation initiation for  $g = 2.54$  cm reflector cone assembly.

shock wave obtained for the reflector plate assembly for the same mixture. Again the higher flame and shock wave velocity measured for the lower  $\beta$  mixture reflects the higher reactivity of the mixture.

The average flame velocity measured along the entire tube is provided in Fig. 7 for four different mixtures. For these mixtures, the flame decelerates in the smooth section of the tube to roughly 500 m/s just before the cone. The measured velocities after the reflector cone assembly for the  $\beta = 4.20$ ,  $\beta = 4.00$ , and  $\beta = 3.80$  mixtures are close to the theoretical CJ detonation velocity of 1900 m/s, which indicates that a detonation wave is initiated as a result of the interaction of the shock wave with the cone reflector assembly. The flame velocity after the assembly for the  $\beta = 4.40$  mixture is well below the theoretical detonation velocity, indicating unsuccessful detonation initiation.

The pressure-time histories recorded by pressure transducers, located at 1.63 and 1.78 m from the ignition point for the  $\beta = 3.80$  mixture and  $\beta = 4.40$  mixture, are shown in Fig. 8. For the  $\beta = 3.80$  mixture (Fig. 8b), the pressure transducer located at 1.63 m shows an initial rapid rise in pressure associated with the incident shock wave to roughly 10 atm. This pressure transducer location roughly corresponds to the axial location of the cone apex. The pressure transient recorded at 1.78 m, located between the base of the cone and the reflecting orifice plate, reveals that the incident shock wave is strengthened across the cone to roughly 14 atm. This overpressure corresponds to a shock wave velocity of 1072 m/s. This initial rise in pressure is followed by a second rapid rise in pressure to 35 atm. This second rise in pressure occurs approximately 30  $\mu$ s after the incident shock pressure rise and corresponds to the passage of the reflected shock wave. Roughly 8  $\mu$ s later, a third sharp rise in pressure to over 65 atm occurs. (Note the signal is clipped.) This strong shock is the result of detonation initiation in the general area

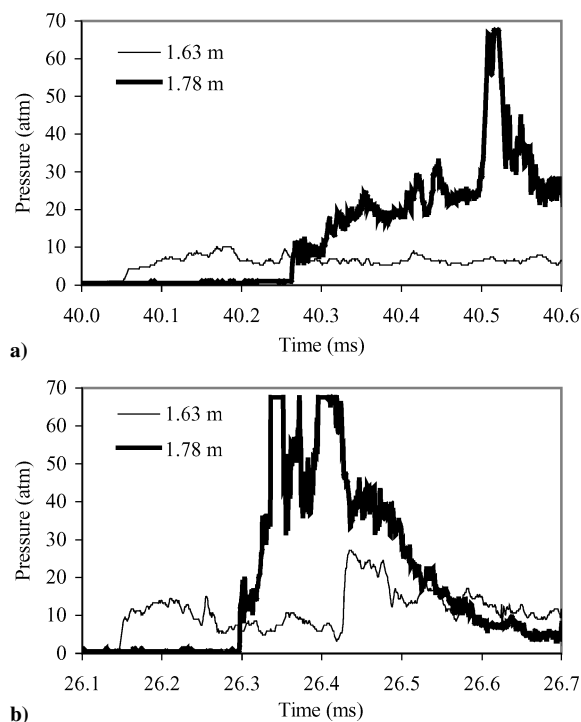


Fig. 8 Pressure time history for the reflector cone assembly with gap spacing of 5.1 cm; test mixture: a)  $\beta = 4.4$  and b)  $\beta = 3.8$ .

of the reflecting orifice plate after the cone. The pressure recorded at 1.63 m shows a second pressure rise to 30 atm, 92  $\mu$ s after the 65-atm spike observed in the 1.78-m pressure transducer. This corresponds to a shock wave with velocity 1700 m/s propagating back toward the cone apex. This velocity magnitude is consistent with a detonation wave. As is the case with the reflector plate, when a detonation is initiated, large pressure oscillations ensue due to the reverberation of the detonation shock wave (Fig. 4b).

The pressure-time history recorded at 1.63 and 1.78 m for the  $\beta = 4.40$  (Fig. 8a) mixture again shows the strengthening of the incident shock wave from roughly 5 to 9 atm. The measured average shock velocity between the pressure transducers is 754 m/s, which is much lower than the observed shock velocity of 1112 m/s for the  $\beta = 3.8$  mixture. A rise in pressure to 65 atm occurs 234  $\mu$ s after the onset of the incident shock wave, this is more than twice the delay observed for the  $\beta = 3.8$  case. The much delayed large-pressure pulse is the result of an explosion in the general area of the assembly. The exact location of this explosion is difficult to ascertain from the limited data available. One can speculate that the explosion occurs in the jet that forms emanating from the orifice plate after the passage of the initial shock. When the flame reaches the turbulent jet, combustion occurs very rapidly, producing a strong shock wave. An explosion may also be triggered in the gas at the tube centerline behind the cone base as a result of the high pressure and temperature produced by the imploding shock. The average shock velocity readings farther down the tube indicate that the flame is moving well below the theoretical detonation velocity. Hence, detonation initiation by shock reflection did not transpire in this situation.

All of the results for the cone assembly are provided in Fig. 9. For a gap spacing of 5.1 cm, detonation was not observed for any value of  $\beta$  down to 3.61, where detonation initiation occurs spontaneously within the flame acceleration section of the tube. For a gap of 2.54 cm, the critical  $\beta$  is 4.33, which is well above the critical value of 3.98 obtained for the reflector plate assembly. For this critical value of  $\beta$ , the average shock velocity measured across the cone was 758 m/s. Clearly, the reflector cone assembly with a gap spacing of 2.54 cm is superior to the plate assembly in terms of initiating a detonation wave in a less reactive mixture.

Table 2 Effect of reducing the flame acceleration distance and orifice plate BR for  $\beta = 3.76$

Reflector position, m	Transition length, m	Flame acceleration orifice plate BR	Shock velocity, m/s	Detonation initiation
1.82	0.46	0.42	1016	Yes
1.67	0.46	0.42	910	Yes
1.52	0.46	0.42	756	Yes
1.36	0.46	0.42	461	No
1.36	0.30	0.42	474	No
1.36	0.30	0.6	771	Yes
1.36	0.30	0.75	710	No

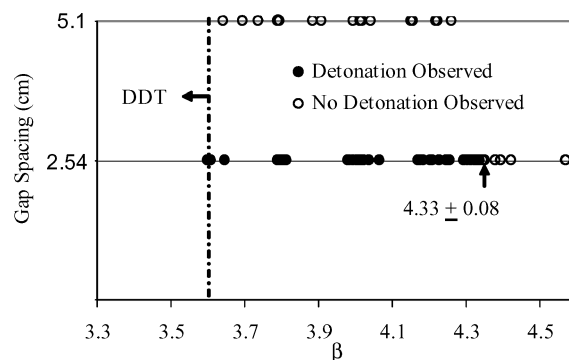


Fig. 9 Detonation initiation results for reflector cone assembly.

#### Effect of Flame Acceleration Section Length on Detonation Initiation

For a PDE application, it is desirable to minimize the combustion tube length to keep the overall engine size as small as possible. A series of experiments was performed to examine the consequences of moving the reflector assembly closer to the ignition point, effectively shortening the flame acceleration section of the tube. The mixture composition used in these tests was stoichiometric ethylene-air ( $\beta = 3.76$ ). The reflector cone assembly with a gap spacing of 2.54 cm was used in these experiments. The distance to the reflector assembly is reduced by removing orifice plates at the end of the flame acceleration section. The results from these experiments are summarized in Table 2. The location of the reflector assembly is given from the ignition endplate to the reflector assembly orifice plate. The data provided in the first row of Table 2 correspond to the  $\beta = 3.8$  test from Fig. 7. This will be considered the baseline case. For this baseline case, the average shock velocity measured across the cone was 1016 m/s and detonation initiation was observed. Detonation initiation was also observed when the reflector assembly was placed 1.67 and 1.52 m from the ignition point. However, when the cone assembly was placed at 1.36 m from the ignition point, detonation initiation was unsuccessful.

From the results in the first four rows of Table 2, it is clear that moving the reflector assembly closer to the ignition point results in a decrease in the strength of the shock wave reaching the cone assembly. For the case where the assembly was located at 1.36 m, the shock wave velocity was only 461 m/s. This corresponds to a reflected shock pressure and temperature of 4.22 atm and 451 K, respectively. This is well below the published "autoignition temperature" for the mixture,<sup>22</sup> which represents the minimum mixture temperature required for the ignition of a flame. Consequently, this temperature is too low to initiate a detonation wave. To prolong the flame acceleration, the orifice plate array was extended by one plate and the length of the transition section was reduced to 0.30 m. This resulted in a slightly stronger shock wave, for example, 474 m/s, but did not result in detonation initiation.

It is clear that a strong shock wave is required to generate the high temperature and pressure required for detonation initiation. With the 0.43 BR orifice plates, it is not possible to accelerate the flame fast enough to produce a strong enough shock wave to initiate a detonation wave when the reflector assembly is located at

1.36 m. However, it is well known that flame acceleration can be enhanced by changing the blockage ratio of the accelerating orifice plates.<sup>6</sup> Additional experiments were performed in which the flame acceleration orifice plate blockage ratio was increased to 0.60 and 0.75 while keeping the cone assembly position at 1.36 m and the transition section length at 0.30 m. With the 0.6 BR orifice plates, a shock velocity of 771 m/s was achieved at the reflector assembly, and for the 0.75 BR plates, a shock velocity of 710 m/s was achieved. Detonation initiation was unsuccessful using the 0.75 BR flame acceleration orifice plates and successful with 0.6 BR flame acceleration orifice plates. The results in Table 2 indicate that for the cone assembly positioned at 1.36 m a minimum average shock velocity across the cone of roughly 750 m/s is required. This critical velocity was also found for the reflector cone assembly experiments performed with the assembly at 1.78 m from the ignition point.

## Discussion

### Reflector Plate Assembly

Based on the experimental results presented, it is clear that the reflector plate promotes detonation initiation because a less reactive mixture can be detonated with the assembly in place than without the assembly present. Unfortunately, the apparatus does not lend itself to visualization to determine the exact nature of the detonation initiation event. However, some insight into the detonation initiation phenomenon can be obtained by analyzing the pressure-time history recorded at the axial position between the reflector plate and orifice plate. In general, there can be up to three distinct large pressure rises resulting from the passage of different shock waves. The first pressure rise is generally associated with the passage of the inert shock wave generated ahead of the flame. The exception to this is for mixtures with  $\beta < 3.61$ , where detonation initiation occurs in the flame acceleration section or the transition section. This shock wave reflects off the reflector orifice plate and arrives at the pressure transducer location a short time after the passage of the incident wave. This second pressure rise may or may not exist depending on if detonation initiation occurs as a result of shock reflection off the plate. The third and largest pressure rise is associated with the shock wave produced by the rapid reaction arising from the shock reflection off the reflector orifice plate. If the conditions are appropriate, this third pressure pulse corresponds to the detonation wave.

For the purpose of this analysis, the explosion induction time  $\tau_E$  is defined as the difference in time of arrival of the incident shock wave and the strong shock wave produced by the rapid reaction. These times are measured at the pressure transducer located between the reflector plate and orifice plate. For detonation initiation to occur in the high-temperature and high-pressure gas adjacent to the reflecting surface, the time that the thermodynamic state is sustained must be on the order of the chemical induction time for the mixture. The temperature and pressure of the gas adjacent to the reflecting surface of a wall-mounted obstacle is reduced by the encroachment of expansion waves originating from the free edge of the reflecting surface. Thus, the time over which the reflected shock temperature and pressure exists is equal to the transit time for an expansion wave to traverse the reflecting surface.<sup>17</sup>

The explosion induction time measured for experiments with the reflector plate assembly is provided in Table 3. Also indicated is whether or not a detonation wave was initiated.

For the configuration tested, there are several opportunities for shock reflection: The first is when the incident shock wave reflects off the face of the circular plate. Because the circular plate has a much larger transverse dimension compared to the flame acceleration orifice plates, the high-temperature and high-pressure gas condition created by the reflection process lasts longer, and as a result, detonation initiation can occur in less reactive mixtures. For the case of detonation initiation occurring at the front surface of the circular plate, the explosion induction time would be very short due to the short transit time for the detonation wave to propagate from the plate to the pressure transducer. This explosion time is mainly governed by the chemical reaction induction time, which dictates how long after shock reflection the detonation wave forms.

**Table 3** Explosion induction time measurements for reflector plate assembly with gap spacing = 5.1 cm

$\beta$	Incident shock velocity, m/s	Measured $\tau_E$ , $\mu$ s	Detonation
3.60	1065	14	Yes
3.83	976	15	Yes
3.78	1022	16	Yes
3.81	951	17	Yes
3.98	964	20	Yes
3.94	1002	152	Yes
3.97	907	157	Yes
4.00	918	139	No
4.01	918	144	No
4.04	880	160	No
4.10	886	173	No
4.21	841	195	No
4.20	865	198	No
4.22	765	299	No

An estimate of the induction time is obtained based on a constant volume chemical reaction process with the initial mixture condition taken to be the normal reflected shock pressure and temperature. The Konnov mechanism<sup>23</sup> with 1027 reactions and 121 species is used for the calculation. For the mixture range of interest, that is,  $\beta$  between 3.6 and 4.0, the chemical induction time varies very little for a given incident shock wave velocity. For this mixture range and incident shock velocities of 950 and 1000 m/s, the calculated induction time is 10 and 30  $\mu$ s, respectively. Taking an average value of 20  $\mu$ s, we can conclude that the explosion induction time for detonation initiation occurring at the front plate is roughly 20  $\mu$ s. The next opportunity for detonation initiation is when the incident shock wave reflects off the reflector orifice plate and also when the shock wave implodes behind the plate. For a detonation wave initiating by either of these mechanisms, the explosion induction time would be significantly longer because the incident shock wave must travel a longer distance to reach the reflection surface, or the tube centerline in the case of shock implosion. Again for a chemical induction time of 20  $\mu$ s, the explosion time for either of these phenomena is estimated to be greater than 100  $\mu$ s.

Recall for mixtures with  $\beta$  less than 3.61, detonation initiation occurs before the reflector assembly and, thus, is not relevant to this analysis. For mixtures in the range  $\beta = 3.61$ –3.98, detonation initiation was observed, and the measured explosion induction times (Table 3) are in the range of 14–20  $\mu$ s. Based on these timescales, it can be concluded that detonation initiation occurs at the front face of the reflector plate. It is not clear if the detonation wave can successfully negotiate the convoluted path through the annulus to the orifice plate hole. If the detonation wave fails during the diffraction process around the plate edge, the decoupled shock wave would then reflect off the reflector orifice plate reinitiating a detonation wave. This detonation wave would then continue through the orifice plate into the latter section of the tube. For the two mixtures  $\beta = 3.94$  and  $\beta = 3.97$ , detonation was observed; however, the observed explosion induction times of 152 and 157  $\mu$ s are much longer than the 20  $\mu$ s for detonation initiation resulting from shock reflection off the plate. Based on this explosion induction time, one can conclude that initiation occurs due to reflection off the orifice plate or implosion of the wave behind the plate. Note that the difference in the time of arrival of the shock wave and the flame at the orifice plate for a  $\beta = 4.0$  mixture is 373  $\mu$ s (Table 1). This time is significantly larger than the explosion time of roughly 150  $\mu$ s recorded for the  $\beta = 3.94$  and  $\beta = 3.97$  tests. Based on the difference in these two times, one can conclude that the flame plays no role in the detonation initiation phenomenon.

For mixtures with  $\beta > 4.0$ , detonation was not observed after the reflector assembly; however, a larger pressure pulse was recorded between the cone and the orifice plate. For these mixtures, the explosion induction time was greater than 160  $\mu$ s, which is consistent with a strong shock wave produced by an explosion occurring as a result of shock implosion.

For a 2.54-cm gap, detonation propagation after the reflector plate assembly was not observed for any mixture. Recall the detonation wave fails as it propagates around the plate producing a decoupled shock flame complex. Re-initiation may occur when the decoupled shock reflects off the reflector orifice plate. This newly formed detonation would then have to propagate through the narrow gap between the back of the reflector plate and the front of the reflector orifice plate. Based on the results for the 2.54-cm gap, this is not possible.

### Cone Assembly

It is believed that the shock dynamics created by the cone is the reason why the cone assembly can detonate weaker mixtures than the reflector plate assembly. As the shock wave propagates through the annulus between the cone and the tube wall, the shock is reflected by the cone surface and the cone deflects the flow behind the shock wave.<sup>12</sup> The cone half-angle in these experiments is 21 deg, which is well below the critical wedge angle of 45 deg for Mach reflection. Whitham's theory,<sup>15</sup> is used to predict the triple-point trajectory angle relative to the cone surface, as well as the Mach stem strength. Once the Mach stem reaches the base of the cone, it diffracts around the corner as shown schematically in Fig. 10. The decrease in shock strength in the diffracted region can be understood as a self-similar, unsteady expansion fan that interacts with the Mach stem. The Mach stem eventually reflects off the tube wall, producing a new Mach stem that propagates parallel to the tube wall. It is this Mach stem that passes over the pressure transducer located at 1.78 m that produces the first sudden rise in pressure (Fig. 8). Ultimately, it is this Mach stem that reflects off the orifice plate initiating a detonation wave. It is of interest to determine if the expansion fan completely overtakes the entire initial Mach stem and the Mach stem created at the tube wall. If the expansion overtakes the wall Mach stem, it will be weakened before it reflects off the orifice plate. The trajectory of the point of intersection of the head of the expansion fan with the undisturbed shock is given by<sup>17</sup>

$$\theta_e = \tan^{-1}(V_w/c) \quad (2)$$

where  $\theta_e$  is the angle separating the disturbance boundary of the incident shock wave (Mach stem) and diffracted shock region, and  $c$  is the acoustic velocity behind the shock front.  $V_w$  is the speed of the boundary for the disturbed region along the shock front, given by the equation

$$V_w = \sqrt{c^2 - (U - u)^2} \quad (3)$$

Table 4 provides a summary for the Mach reflection calculations for the cone reflector geometry. The axial distance  $X$  before the

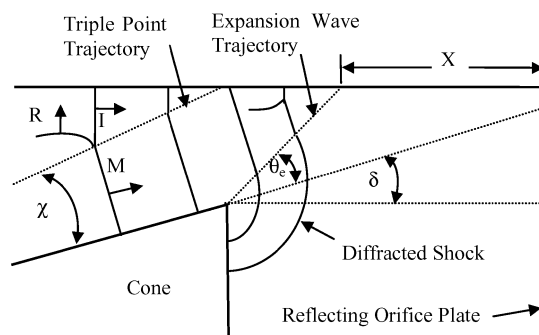


Fig. 10 Shock diffraction of Mach stem around the cone: I, incident wave; M, Mach stem; and R, reflected wave.

reflector orifice plate, where the entire Mach stem is affected by the expansion fan (Fig. 10) is provided in the last column of Table 4. Based on the calculations, for both the 2.54 and 5.1-cm gap, the Mach stem does not arrive at the reflector orifice plate without being attenuated by the expansion fan. (See the values of  $X$  in Table 4.) For a gap spacing of 5.1 cm, the decaying Mach stem has a much farther distance to travel to the orifice plate where shock reflection occurs and, thus, is less likely to result in detonation initiation. This attenuation explains why detonation initiation is successful for a gap of 2.54 cm and unsuccessful for the cone reflector assembly with a gap of 5.1 cm. The attenuation process of the wall Mach stem requires significant numerical modeling, which is beyond the scope of this study.

### Conclusions

It was found that detonation initiation occurs spontaneously in the orifice plate laden tube used in this study for mixtures of ethylene-oxygen with nitrogen dilution yielding  $\beta < 3.61$ . Experiments involving a reflector plate followed by an orifice plate with a gap of 5.1 cm have shown success with regards to initiating detonations by means of shock reflection. With the reflector assembly in place, mixtures with a  $\beta$  value up to 3.98 were successfully detonated. The plate provides a larger surface area for shock reflection and, thus, sustains the reflected gas temperature for a longer time compared to the orifice plate alone. For the 2.54-cm gap case, detonation was not observed. One can surmise that the distance separating the plate and the reflecting orifice plate is less than the critical detonation initiation kernel size. For the smaller gap, CJ level pressures were measured within the vicinity of the obstacle, but initiation ultimately was unsuccessful.

Experiments performed with the reflector cone assembly demonstrated the shock strengthening produced by the area reduction resulted in detonation initiation in less reactive mixtures compared to the plate assembly. Mixture compositions up to  $\beta = 4.33$  were detonated. It is proposed that the shock wave strengthens as it propagates through the annulus around the cone leading up to the reflecting orifice plate. With use of the cone reflecting assembly, experiments were performed with stoichiometric ethylene-air where the cone assembly was moved successively closer to the point of ignition. Detonation initiation was observed with the reflector cone assembly at 1.36 m from ignition point using flame acceleration orifice plates with a blockage ratio of 0.60. A 1.36-m-long combustor is approaching a practical size for a functional PDE.

### Acknowledgments

This work was made possible through financial support from Defence Research and Development of Canada-Suffield.

### References

- Eidelman, S., Grossmann, W., and Lottati, I., "Review of Propulsion Applications and Numerical Simulations of Pulse Detonation Engine Concept," *Journal of Propulsion and Power*, Vol. 7, No. 7, 1991, pp. 857-865.
- Kailasanath, K., "Review of Propulsion Applications of Detonation Waves," *AIAA Journal*, Vol. 38, No. 9, 2000, pp. 1698-1708.

Table 4 Mach reflection calculations for the reflector cone assembly

$\beta$	Incident shock velocity, m/s	Incident Mach number	Mach stem Mach number	Distance from reflecting orifice plate X, cm
Gap = 5.1 cm				
3.64	1137	3.45	4.14	2.96
3.69	1219	3.70	4.44	2.94
3.79	1058	3.21	3.85	2.98
3.80	1073	3.26	3.91	2.98
4.00	952	2.89	3.46	3.01
4.02	946	2.87	3.44	3.02
4.22	896	2.72	3.25	3.04
4.26	846	2.57	3.08	3.05
Gap = 2.54 cm				
3.60	1112	3.38	4.06	0.41
3.79	1029	3.13	3.75	0.43
3.81	1051	3.19	3.80	0.42
3.99	935	2.84	3.40	0.46
4.17	896	2.72	3.25	0.48
4.17	876	2.66	3.18	0.48
4.35	758	2.30	2.73	0.54
4.42	751	2.28	2.71	0.54



- <sup>3</sup>Roy, G. D., Frolov, S. M., Borisov, A. A., and Netzer, D. W., "Pulse Detonation Propulsion: Challenges, Current Status, and Future Perspective," *Progress in Energy and Combustion Science*, Vol. 30, No. 6, 2004, pp. 545–672.
- <sup>4</sup>Heisser, W. H., and Pratt, D. T., "Thermodynamic Cycle Analysis of Pulse Detonation Engines," *Journal of Propulsion and Power*, Vol. 18, No. 5, 2002, pp. 68–76.
- <sup>5</sup>Pinard, P., Higgins, A., Lee, J. H., and Murray, S. B., "The Effect of NO<sub>2</sub> Addition on Deflagration-to-Detonation Transition," *Combustion and Flame*, Vol. 136, No. 1–2, 2004, pp. 146–154.
- <sup>6</sup>Ciccarelli, G., Fowler, C. J., and Bardon, M., "Effect of Obstacle Size and Spacing on the Initial Stage of Flame Acceleration in a Rough Tube," *19th International Colloquium on the Dynamics of Explosive and Reactive Systems Shock Waves*, 2003 (accepted for publication).
- <sup>7</sup>Lee, S. Y., Watts, J., Saretto, S., Pal, S., Conrad, C., Woodward, R., and Santoro, R., "Deflagration to Detonation Transition Process by Turbulence-Generating Obstacles in Pulse Detonation Engines," *Journal of Propulsion and Power*, Vol. 20, No. 6, 2004, pp. 1026–1036.
- <sup>8</sup>Cooper, M., Jackson, S., Austin, J., Wintenberger, E., and Shepherd, J. E., "Direct Experimental Impulse Measurements for Detonations and Deflagrations," *Journal of Propulsion and Power*, Vol. 18, No. 5, 2002, pp. 1033–1041.
- <sup>9</sup>Strehlow, R. A., and Cohen, R., "Initiation of Detonation," *Physics of Fluids*, Vol. 5, No. 1, 1982, pp. 97–101.
- <sup>10</sup>Lee, J. H. S., Knystautas, R., and Chan, C. K., "Turbulent Flame Propagation in Obstacle-Filled Tubes," *Proceedings of the Combustion Institute*, Vol. 20, 1985, pp. 1663–1672.
- <sup>11</sup>Moen, I. O., Donato, M., Knystautas, R., and Lee, J. H., "Flame Acceleration Due to Turbulence Produced by Obstacles," *Combustion and Flame*, Vol. 39, No. 1, 1980, pp. 21–32.
- <sup>12</sup>Ben-Dor, G., and Glass, I. I., "Domains and Boundaries of Non Stationary Oblique Shock Wave Reflexions. 1. Diatomic Gas," *Journal of Fluid Mechanics*, Vol. 92, 1979, pp. 459–496.
- <sup>13</sup>Hornung, H., "Regular and Mach Reflection of Shock Waves," *Annual Review of Fluid Mechanics*, Vol. 18, 1986, pp. 33–58.
- <sup>14</sup>Yang, J., Sasoh, A., and Takayama, K., "The Reflection of a Shock Wave over a Cone," *Shock Waves*, Vol. 6, No. 5, 1996, pp. 267–273.
- <sup>15</sup>Whitham, G. B., "A New Approach to the Problem of Shock Dynamics, Part 1. Two-Dimensional Problems," *Journal of Fluid Mechanics*, Vol. 2, 1957, pp. 145–171.
- <sup>16</sup>Chan, C., "Collision of a Shock Wave with Obstacles in a Combustible Mixture," *Combustion and Flame*, Vol. 100, No. 1–2, 1995, pp. 341–348.
- <sup>17</sup>Thomas, G., Ward, S., Williams, R., and Bambrey, R., "On the Critical Condition for Detonation Initiation by Shock Reflection from Obstacles," *Shock Waves*, Vol. 12, No. 2, 2002, pp. 111–119.
- <sup>18</sup>Gelfand, B. E., Khomik, S. V., Bartenev, A. M., Medvedev, S. P., Grönig, H., and Olivier, H., "Detonation and Deflagration Initiation at the Focusing of Shock Waves in Combustible Gaseous Mixture," *Shock Waves*, Vol. 10, No. 3, 2000, pp. 197–204.
- <sup>19</sup>Jackson, S. I., and Shepherd, J. E., "Detonation Initiation Via Imploding Shock Waves," AIAA Paper 2004-3919, 2004.
- <sup>20</sup>Li, C., and Kailasanath, K., "Detonation Initiation by Annular-Jet-Induced Imploding Shocks," *Journal of Propulsion and Power*, Vol. 21, No. 1, 2005, pp. 183–186.
- <sup>21</sup>Knystautas, R., Lee, J. H., Peraldi, O., and Chan, C. K., "Transmission of a Flame from a Rough to a Smooth-Walled Tube," *Dynamics of Explosions*, Vol. 106, Progress of Astronautics and Aeronautics, AIAA, New York, 1986, pp. 37–52.
- <sup>22</sup>Glassman, I., *Combustion*, Academic Press, London, 1977, p. 596.
- <sup>23</sup>Konnov, A. A., "Development and Validation of a Detailed Reaction Mechanism for the Combustion Modeling," *Eurasian Chemico-Technological Journal*, Vol. 2, 2000, pp. 257–264.